



## Formulation development of medicated chewing gum tablets by direct compression using the SeDeM-Diagram-Expert-System



Lisa Zieschang<sup>a,b</sup>, Martin Klein<sup>b</sup>, Nathalie Jung<sup>a</sup>, Johannes Krämer<sup>c</sup>, Maike Windbergs<sup>a,\*</sup>

<sup>a</sup> Institute of Pharmaceutical Technology and Buchmann Institute for Molecular Life Sciences, Goethe-University Frankfurt, Max-von-Laue-Str. 15, 60438 Frankfurt am Main, Germany

<sup>b</sup> PHAST Development GmbH & Co. KG, Byk-Gulden-Str. 2, Campus Konstanz, 78467, Germany

<sup>c</sup> DISSO GmbH, Preussenstr. 15, 66424 Homburg, Germany

### ABSTRACT

Medicated chewing gums represent an orally administered dosage form with promising potential for local and systemic drug delivery. However, compared to other solid oral dosage forms, formulation development and release mechanism of medicated chewing gums are extremely complex, and thus only few products reached the approval for the market so far. Therefore, Quality by Design (QbD) approaches for rational formulation development of medicated chewing gums are needed to utilize their full potential. For chewing gum tablets, which are manufactured by direct compression, QbD approaches derived from tableting processes might be exerted. In this context, the SeDeM-Diagram-Expert-System implements the QbD approach while indicating whether a blend is suitable for direct compression and comprises powder properties, which need to be improved to facilitate the formulation development. Here, we present the successful application of the SeDeM-Diagram-Expert-System to the formulation development of medicated chewing gum tablets manufactured by direct compression. Furthermore, limitations of the SeDeM-System for medicated chewing gum tablets are evaluated and potential modifications of the system are suggested and discussed for future use.

### 1. Introduction

Medicated chewing gums (MCG) represent a desirable dosage form for drug delivery which proves to be advantageous compared to other orally administered drug products, due to the simple administration and high patient compliance, as well as the avoidance of the hepatic first-pass effect by buccal absorption of the active pharmaceutical ingredient (API). Despite those beneficial characteristics and the possibility of incorporating locally and systemically acting substances, only few drug products exist on the market so far [1–5]. The low abundance of marketed MCG is due to the complexity of manufacturing and the challenging development of tests for quality and performance to assure a high quality product [2,6]. Especially the unique release mechanism of the drug substance from the gum matrix by mastication needs to be considered already at the stage of selecting the manufacturing method [7–11]. MCG are most commonly manufactured by using the traditional hot melting/extrusion method, which includes heating of the gum base, addition of API and excipients, followed by cutting the chewing gums into pieces after cooling. This method is time consuming and of limited use for substances sensitive to moisture and heat. To overcome these restrictions, direct compression of powdery gum base mixtures poses an innovative alternative for the incorporation of sensitive molecules like proteins into chewing gum tablets [7,12]. Direct compression is a common manufacturing process used for tablets, but the formulation

development can be challenging due to insufficient flow and tableting properties of the bulk material, limited loading capacities as well as segregation problems of the powder [13]. The current “Quality by Design ICH 8” concept (QbD) suggests, among the characterisation of critical process parameters (CPPs), also a systematic physicochemical characterisation of the API and the excipients (critical material attributes; CMAs), aiming for identification and understanding of key aspects which influence the quality of the final product. By combining those two parameters, a design space can be estimated to meet the specifications given by the critical quality attributes (CQAs) derived from the quality target product profile (QTPP) [14]. In this context, the SeDeM-Diagram-Expert-System (SeDeM-System) was established as a tool in the QbD approach for optimised formulation development of tablets. The SeDeM-System can be applied to a systematic investigation of the CMAs represented by five critical factors affecting the tableting process [15]. According to Suñé-Negre et al. these five factors comprise dimensions of the bulk material, compressibility and flowability of the powder as well as the lubricity, on the one hand with respect to stability and on the other hand with respect to dosage of the product. The experiments are based on 12 pharmacopoeial methods and established experimental procedures. Consecutively, the results of the powder characterisation are normalised, presented in a polygonal radar-chart and the values are translated into acceptance indexes. The combination of data reduction and illustration facilitates formulation development

\* Corresponding author.

E-mail address: [windbergs@em.uni-frankfurt.de](mailto:windbergs@em.uni-frankfurt.de) (M. Windbergs).

<https://doi.org/10.1016/j.ejpb.2019.09.003>

Received 15 April 2019; Received in revised form 23 August 2019; Accepted 3 September 2019

Available online 04 September 2019

0939-6411/ © 2019 Elsevier B.V. All rights reserved.

and optimisation for manufacturing of tablets using direct compression, since it evaluates CMAs of the active pharmaceutical ingredient (API) and excipients as well as the properties of the complete blend. Furthermore, batch-to-batch reproducibility and optimisation of formulation development can be supported by saving time and resources [16–18]. Apart from successful formulation development of tablets for direct compression, the SeDeM-System has been applied and adjusted to other solid oral dosage forms, manufactured by direct compression [19–22]. The manufacturing of chewing gum tablets is identical to the direct compression approach for tablets. Therefore, parameters influencing the rheological properties of tablet formulations are expected to show the same impact on chewing gum tablets, although the QTPP of both dosage forms is different. The QTPP of MCG is described in the Ph. Eur. as “[...] solid, single-dose preparations with a base consisting mainly of gum that are intended to be chewed but not swallowed.” [8]. Against this background, the objective of this study was to investigate the applicability of the SeDeM-System for the formulation and manufacturing of MCG by direct compression. Especially the adaptability of the different SeDeM-System parameters for the testing of powdery chewing gum blends was evaluated and discussed. The protein lysozyme was chosen as a model API, sensitive to moisture and heat, with the preference for direct compression to be used for manufacturing of lysozyme loaded MCG. The sensitivity of the SeDeM-System for formulation changes was tested with an initial mixture of gum base and excipients, loaded with 5% lysozyme. The formulation parameters particle size distribution and lysozyme loading were systematically altered and the results were compared. The discrepancy between the results of SeDeM characterisation and the requirements for chewable MCG is discussed in the context of parameters to be included in a characterisation system suitable for this dosage form.

## 2. Materials and methods

### 2.1. Materials

Lyophilized lysozyme (Bioseutica, Zeewolde, Netherlands) (purity > 98%) was used as API in combination with the gum base “Health in Gum PWD-03” (Cafosa, Barcelona, Spain). Excipients to improve powder characteristics were highly dispersible silicon dioxide as glidant and magnesium stearate as lubricant (both Merck KGaA, Darmstadt, Germany).

### 2.2. Methods

#### 2.2.1. SeDeM-Diagram-Expert-System

The SeDeM-System was originally described by Suñé-Negre et al. with the first publication in 2005 and applies the QbD concept to the formulation development of tablets manufactured by direct compression by investigating CMAs and connects the information to the CQAs of the drug product to meet the QTPP [15]. The CQAs for tablets manufactured by direct compression include product purity, strength, drug release and stability [14]. These aspects are partly covered by the SeDeM-System by correlating the strength, preferably the mechanical stability, and the product stability, after testing different parameters to characterise the raw powders and the blends [15]. Even the prediction of drug release has been successfully demonstrated for orally disintegrating tablet formulations with the SeDeM-ODT-System [20]. The main focus of the SeDeM-System is the facilitated formulation development of dosage forms, manufactured by direct compression. In this context, the predominant factor for the formulation development is the influence of the input material on the final drug product. The SeDeM-System provides a basis for the systematic investigation of CMAs with focus on the suitability of the powdered substance for direct compression and the mechanical stability of the final drug product.

By investigating the drug substance according to the SeDeM-System, properties with negative influence on the mechanical stability of the

tablet can be identified and excipients (including their quantitative ratio in the formulation) to compensate these characteristics can be selected accordingly [17,23]. The successful implementation of the SeDeM-System in the formulation development has been shown in several publications, however potential shortcomings of the system have been discussed as well [24,25]. Limits of the SeDeM-System are due to the formal assumption of a linear behaviour in a disordered system consisting of different substances. Scholtz et al. investigated the predictability of the amount of excipients required to manufacture blends with different drug substances, which are suitable for direct compression. In case the prediction failed, the authors identified a possible cause for the non-linear behaviour of the blend. The physico-chemical properties, like adhesive behaviour of the drug substance, could lead to interactive mixtures. Especially drug substance particles < 100 µm are more likely to interact with surfaces of larger excipient particles and are suspected to form a coating on them, which can mask their properties. The blend properties are then predominantly determined by the smaller particles, although the total amount in the blend is lower than the one of the larger particles [13,24]. The threshold, where the blend characteristics underlie a sudden change, can be explained by the percolation theory. Galdón et al. applied the percolation theory to the SeDeM-System and confirmed the existence of two critical points (drug and excipient percolation threshold). At these two thresholds the blend is subject to abrupt changes in the rheological properties, especially the flow capacity [25]. For a detailed overview about the development of the SeDeM-System and application the reader is referred to Dai et al. [26].

After conducting the experiments, the results of 12 test methods are subjected to a subsequent data reduction to represent the data as SeDeM-Diagram and demonstrate the suitability for the powder to be directly compressible by numerical values of the acceptance indexes. According to the SeDeM-System, powders with acceptance indexes below 3 are not suitable for direct compression at all, between 3 and 5 direct compression is possible by incorporating certain amounts of excipients to improve deficient powder properties and indexes above 5 indicate the suitability for direct compression. Furthermore, the individual ingredients and blends can be compared with the SeDeM-Diagram, to reveal particular deficient powder characteristics, which need to be improved. Either the arithmetic mean value of the parameters grouped into five incidence factors or the *r* values of the individual tested parameter can be used to assess the powder properties. According to that, the following procedures and calculations were performed as originally published [17]. The test values (*v*) of the 12 experiments were normalised by converting them to radius values (*r*), ranging from 0 to 10 (Table 1). The converted data were then visualized as radar-chart. The *r* values indicate whether a powder shows satisfactory (10) or deficient (0) properties for one particular tested parameter, with increasing numbers of *r* values above 5, indicating a higher probability of the powder to be suitable for direct compression. The acceptance indexes parameter index (IP), parameter profile index (IPP) and good compressibility index (IGC), providing an estimator for direct compressibility, were calculated based on the previously determined *r* values (Eq. (1)–(3)). The acceptance criterion of the IP is 0.5, calculated by Eq. (1). Powders with an IP below are not suitable for direct compression [17].

$$IP = \frac{n_{P \geq 5}}{n_{Pt}} \quad (1)$$

where

$$n_{P \geq 5} = \text{Number of parameters with values equal or higher 5}$$

$$n_{Pt} = \text{total number of parameters studied}$$

The acceptance criterion for IPP was calculated with Eq. (2) and for IGC with Eq. (3). Powders with an IPP and IGC below 3 are not suitable for direct compression, values from 3 to 5 suggest the use of excipients

**Table 1**

**Parameters and calculations of the SeDeM-Diagram-Expert-System [16].** Equation for test results to calculate the value (v), acceptance limits of the value and conversion factor applied to v to calculate value r for the SeDeM-Diagram are shown; as well as the equation to calculate the acceptance indexes for the evaluation of the powdered substance and formulation and the reliability factor to use to calculate the acceptance indexes for a polygon with 11 or 12 parameters.

Incidence factor	Parameter	Symbol	Unit	Equation	Acceptable range	Factor applied to value (v)
Dimension	bulk density	Da	g/mL	Da = P/Va	0–1 g/mL	10v
	tapped density	Dc	g/mL	Dc = P/Vc	0–1 g/mL	10v
Compressibility	inter-particle porosity	Ie	–	Ie = Dc – Da/Dc × Da	0–1.2	10v/1.2
	Carr index	IC	%	IC = (Dc – Da/Dc)100	0–50%	v/5
	cohesion index	Icd	N	experimental	0–200 N	v/20
Flowability/powder	Hausner ratio	IH	–	IH = Dc/Da	3–1	(30-10v)/2
	angle of repose	α	°	tg α = h/r	50–0°	10-(v/5)
	powder flow	t <sup>4</sup>	s	experimental	20–0 s	10-(v/2)
Lubricity/stability	loss on drying	%HR	%	experimental	0–10%	10-v
	hygroscopicity	%H	%	experimental	20–0%	10-(v/2)
Lubricity/dosage	Particles < 50 μm	%Pf	%	experimental	50–0%	10-(v/5)
	homogeneity index	*Iθ	–	Iθ = Fm/100 + ΔFmn	0–2 × 10–2	500v
Parameter index		IP		IP = (n <sup>3</sup> P ≥ 5)/n <sup>3</sup> Pt	≥ 0.5	
Parameter profile index		IPP		IPP = Σ r/nr	≥ 5	
Good compressibility index		IGC		IGC = IPP × f	≥ 5	
Reliability factor		f		f = polygon area/circle area	0.952	Polygon with 12 sides
					0.947	Polygon with 11 sides

to improve deficient powder properties and values above 5 indicate suitable characteristics for direct compression [17].

$$IPP = \frac{\sum r}{nr} \quad (2)$$

where

$$\sum r = \text{sum of radius values studied}$$

$$nr = \text{number of radius values studied}$$

$$IGC = IPP \cdot f \quad (3)$$

where

$$f = \text{reliability factor} = \frac{\text{circle area}}{\text{polygon area}} \quad (4)$$

The reliability factor is 0.952 for a 12 sided polygon, specified by the SeDeM-System and 0.947 calculated for an 11 sided polygon [17].

**2.2.1.1. Preparation of the blends.** Cafosa Health in Gum PWD-03 (Cafosa 03) was sieved through a 1 mm sieve before testing and preparing the blends. Highly dispersible silicon dioxide and magnesium stearate were sieved through a 710 μm sieve prior to blend preparation, respectively. Blending of 320 g batches was performed using a Turbula mixer (WAB T2C, Willy A. Bachofen, Basel, Switzerland). The composition of each investigated formulation, expressed in percentage of mass, was as follows:

- formulation 1: Cafosa 03 92%, lysozyme 5%, silicon dioxide 1%, magnesium stearate 2%
- formulation 2: Cafosa 03 (with a particle size distribution of 100 – 355 μm) 92%, lysozyme 5%, silicon dioxide 1%, magnesium stearate 2%
- formulation 3: Cafosa 03 82%, lysozyme 15%, silicon dioxide 1%, magnesium stearate 2%
- placebo formulation: Cafosa 03 97%, silicon dioxide 1%, magnesium stearate 2%

Unless otherwise specified, the particle size of Cafosa 03 was < 1000 μm and for lysozyme d85 < 100 μm. All components, except for magnesium stearate, were mixed for 8 min at 31.5 rpm in the Turbula mixer. After adding magnesium stearate, the blend was mixed for additional 8 min at 31.5 rpm to assure optimal lubrication during the

tableting process. Before each test, the blends were sieved through a 1 mm sieve to break up agglomerates. Every test was carried out in triplicate, unless otherwise specified.

**2.2.1.2. Bulk density (Da).** The calculation of the bulk density (Da) of the individual powders and formulations was performed by determination of the powder volume (100 g) in a graduated cylinder according to the method described in the Ph. Eur. Chapter 2.9.34 [27].

**2.2.1.3. Tapped density (Dc).** The calculation of the tapped density (Dc) of the individual powders and formulations was performed by determination of the powder volume (100 g) in a graduated cylinder after 2500 taps, to obtain maximum packing, with the PT-TD1 (Pharma Test GmbH, Hainburg, Germany) according to the method described in the Ph. Eur. Chapter 2.9.34 [17,27].

**2.2.1.4. Inter-particle porosity (Ie).** The inter-particle porosity (Ie) of the individual powders and formulations is calculated from Da and Dc using Eq. (5) [17]:

$$Ie = Dc - \frac{Da}{Dc} \cdot Da \quad (5)$$

**2.2.1.5. Carr index (IC).** The Carr index (IC) of the individual powders and formulations is calculated from Da and Dc using Eq. (6) [17,27,28]:

$$IC = \frac{Dc - Da}{Dc} \cdot 100 \quad (6)$$

**2.2.1.6. Cohesion index (Icd).** Each individual powder and each formulation was compressed in an eccentric press from Kilian KS (Romaco Kilian GmbH, Cologne, Germany) with the maximum possible compression force for each powder to produce tablets. The punch diameter was 18 mm and the tablet height 2.8 ± 0.3 mm. Six individual tablets were determined with the breaking strength tester HT1 (Sotax GmbH, Lörrach, Germany). The mean value of the hardness (N) was used as cohesion index (Icd) [29].

**2.2.1.7. Hausner ratio (IH).** The Hausner ratio (IH) of the individual powders and formulations was calculated from Da and Dc using Eq. (7) [17,27,28,30]:

$$IH = \frac{Dc}{Da} \quad (7)$$

**2.2.1.8. Angle of repose ( $\alpha$ ).** The angle of repose ( $\alpha$ ) of the individual powders and formulations was determined by the Granulate Flow Tester GTB (Erweka GmbH, Heusenstamm, Germany) using a stainless steel hopper with a diameter of 10 mm of the outlet nozzle. The powder was flowing through the nozzle on a base with fixed diameter according to the Ph. Eur. Chapter 2.9.36 [28]. If no flow or no forming of a cone with a 10 mm, 15 mm or 25 mm nozzle has been observed, the angle of repose was excluded from the SeDeM-Diagram.

**2.2.1.9. Flowability ( $t''$ ).** The flowability ( $t''$ ) of the individual powders and formulations was determined by the Granulate Flow Tester GTB (Erweka GmbH, Heusenstamm, Germany) using a stainless steel hopper with a diameter of 10 mm of the outlet nozzle, according to the Ph. Eur. Chapter 2.9.16. The flowability is expressed as seconds per 100 g of a powder flowing through an orifice [31].

**2.2.1.10. Loss on drying (%HR).** The loss on drying (%HR) of the individual powders and formulations was determined with the moisture analyser HB43 Halogen (Mettler Toledo, Gießen, Germany). About 3 g of the sample was exactly weighed and heated up to 148 °C until constant weight.

**2.2.1.11. Hygroscopicity (%H).** The hygroscopicity (%H) of the individual powders and formulations was calculated from the percentage increase in sample weight after storage in a humidifier at a relative humidity of 76% (saturated sodium chloride solution) and a temperature of  $22 \pm 2$  °C for 24 h [17].

**2.2.1.12. Percentage of particles smaller than 50  $\mu$ m (%PF).** The percentage of particles smaller than 50  $\mu$ m (%PF) of the individual powders and formulations was determined by sieving a suitable amount of the powder through a 50  $\mu$ m sieve by vibrating with the test sieve shaker Haver EML 200 Premium (Haver & Boecker, Oelde, Germany) with an amplitude of 1.5 mm. The percentage of particles passed through the sieve was calculated [16].

**2.2.1.13. Homogeneity index ( $I\theta$ ).** The homogeneity index ( $I\theta$ ) was calculated after classifying 100 g of the individual powders and formulations by using the test sieve shaker Haver EML 200 Premium (Haver & Boecker, Oelde, Germany) with an amplitude of 1.5 mm. The percentage of the powder retained on each sieve was determined and Eq. (8) was applied to the data obtained to calculate the homogeneity index [16]. The sieve sizes used were as follows: 1000  $\mu$ m, 710  $\mu$ m, 500  $\mu$ m, 355  $\mu$ m, 212  $\mu$ m, 100  $\mu$ m, 50  $\mu$ m. The particle size distribution is assumed to be Gaussian, therefore the major fraction complies to the fraction between 212  $\mu$ m and 355  $\mu$ m [17].

$$I\theta = \frac{F_m}{100 + (dm - dm_{-1})F_{m-1} + (dm_{+1} - dm)F_{m+1} + (dm - dm_{-2})F_{m-2} + (dm_{+2} - dm)F_{m+2} + (dm - dm_{-3})F_{m-3} + (dm_{+3} - dm)F_{m+3}} \quad (8)$$

where

$I\theta$  = relative homogeneity index. Particle-size homogeneity in the range of the fractions under study;

$F_m$  = percentage of particles in the majority range;

$F_{m-1}/F_{m-2}/F_{m-3}$  = percentage of particles in the range below the majority range;

$F_{m+1}/F_{m+2}/F_{m+3}$  = percentage of particles in the range above the majority range;

$dm$  = mean diameter of the particles in the majority fraction;

$dm_{-1}/dm_{-2}/dm_{-3}$  = mean diameter of the particles in the fraction of

the range below the majority range;

$dm_{+1}/dm_{+2}/dm_{+3}$  = mean diameter of the particles in the fraction of the range above the majority range.

## 2.2.2. Visualisation and characterisation of the powder

**2.2.2.1. Stereo microscopy.** Small amounts of the individual powders and formulations were placed on the microscope slide of a stereo microscope Stemi 2000-C (Carl Zeiss Microscopy GmbH, Jena, Germany) and illuminated by a KL 1500 LCD (Carl Zeiss Microscopy GmbH, Jena, Germany). Images were recorded by a Canon EOS M50 camera (Canon Europa N.V., Amstelveen, Netherlands).

**2.2.2.2. Variable pressure scanning electron microscopy (VPSEM).** Samples of the individual powders and formulations were fixed to stubs and any loose powder was gently removed. After sample preparation, the samples were transferred in the scanning electron microscope Quanta 200 (FEI Deutschland GmbH, Frankfurt, Germany). The chamber pressure was 60 Pa and a solid state back scattered electron detector was used with an accelerating voltage of 12.5 kV. The spot size was set to 6.0 for the electron beam and images were taken with the FEI software xT microscope Control (version 2.4.).

**2.2.2.3. Confocal Raman microscopy.** All Raman data were attained using an Alpha 300R+ confocal Raman microscope (WITec GmbH, Ulm, Germany) equipped with a 532 nm laser. The laser power was adjusted to 20–40 mW, depending on fluorescence background emitted from the respective samples. A pinhole of 50  $\mu$ m was chosen to exclude signals from out of focus planes. Single Raman spectra of reference substances were acquired using an integration time of 0.5 s and 10 accumulations per spectrum. At least 5 single spectra of a reference substance were used to calculate an averaged Raman spectrum for the respective reference substance (Fig. S2). For the analysis of chewing gum samples, topography maps of single particles of the individual compounds and formulations or compressed chewing gums were acquired using white light reflectance to enable the acquisition of Raman scans of the sample surface. For single particle analysis, scans were recorded with an integration time of 0.4 s per spectrum and a resolution of 1.0  $\mu$ m. Scans of whole chewing gum tablets were recorded using an integration time of 1.0 s per spectrum and a resolution of 50–100  $\mu$ m.

Raman spectra were processed within the WITec software ProjectFOUR by applying cosmic ray removal and a background subtraction procedure using the 'shape' function (100 points). Raman scans were further analysed by hierarchical cluster analysis to map the distribution of lysozyme on the samples. In subsequent basis analysis, the distribution of lysozyme was visualised in false-colour images by depicting the API in yellow and the chewing gum base in a blue colour.

## 2.2.3. Manufacturing and evaluation of chewing gum tablets

**2.2.3.1. Tableting.** The formulations were compressed in an eccentric press from Kilian KS (Romaco Kilian GmbH, Cologne, Germany) with a compression force of approximately 5.25 on the scale of the tableting machine (scale from 1 to 12, with a maximum compression force of 25 kN), filling depth of approximately 9 mm and a punch diameter of 18 mm.

**2.2.3.2. Content analysis.** Six individual chewing gum tablets of each formulation were analysed in parallel. Each chewing gum was transferred in a 125 mL plastic container and mortared until it was powdery again. After adding 15 mL of phosphate buffer pH 6.0 R2, according to the Ph. Eur. [32], the mix was shortly stirred at room temperature (RT) with the pestle. The pestle was rinsed additionally with 15 mL of phosphate buffer pH 6.0 and the solution was vigorously shaken by hand. Immediately after shaking, 2.5 mL of the liquid was sampled with a plastic syringe and filtered through regenerated cellulose filters (pore size 0.22  $\mu$ m, diameter 13 mm, Spartan,

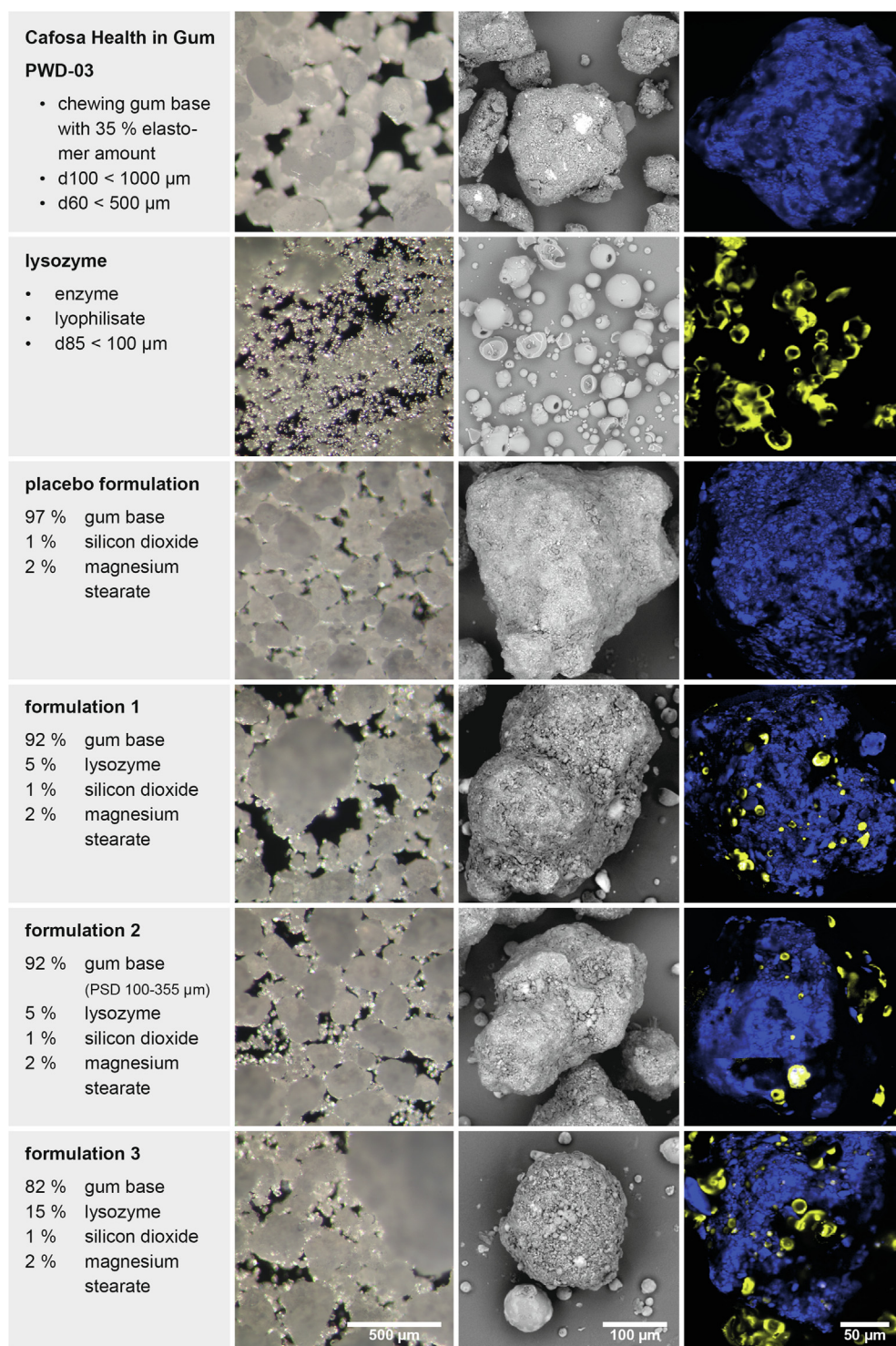


**Fig. 1.** Stereo microscope, variable pressure scanning electron microscope (VPSEM) and confocal Raman microscope images of the powdered substances and formulations. Comparison of the chewing gum base Cafosa HiG PWD-03, lysozyme, placebo formulation, as well as formulation 1, 2 and 3, with the Stereo-microscope (2. column) at 2.5x magnification and VPSEM (3. column) at 500x magnification. Adhesive lysozyme (yellow) on the gum base blend with excipients (blue) was visualized by the chemically selective analysis by confocal Raman microscopy (4. column). PSD = particle size distribution. (For interpretation of the references to colour in this figure legend, the reader is referred to the web version of this article.)

Whatmann), conditioned with 1 mL sample solution. The sample solutions of formulations 1 and 2 were analysed directly. The sample solutions of formulation 3 were diluted 1:3 with phosphate buffer pH 6.0 before the analysis. Quantification of released lysozyme was done using high performance liquid chromatography (HPLC) described in Section 2.2.3.6.

**2.2.3.3. Friability.** The friability test was performed as described in the Ph. Eur. Chapter 2.9.7. Each formulation was tested in three repetitions with 10 specimens each. The chewing gums were dedusted, weighed and transferred into the drum of the friability tester TA 200 (Erweka

GmbH, Heusenstamm, Germany). After 100 rotations at 25 rpm, the chewing gums were dedusted and weighed again. The difference in weight was expressed in percentage and is specified to be less than 1%. The test was considered to be failed if damaged tablets were present [33].

**2.2.3.4. Resistance to crushing.** Ten individual chewing gum tablets were determined using the breaking strength tester HT1 (Sotax GmbH, Lörrach, Germany). The test mode was set to constant speed of 1 mm/s and a sensitivity of 1% to determine the critical point of fracture. After aligning the tablets horizontally, the radial force was

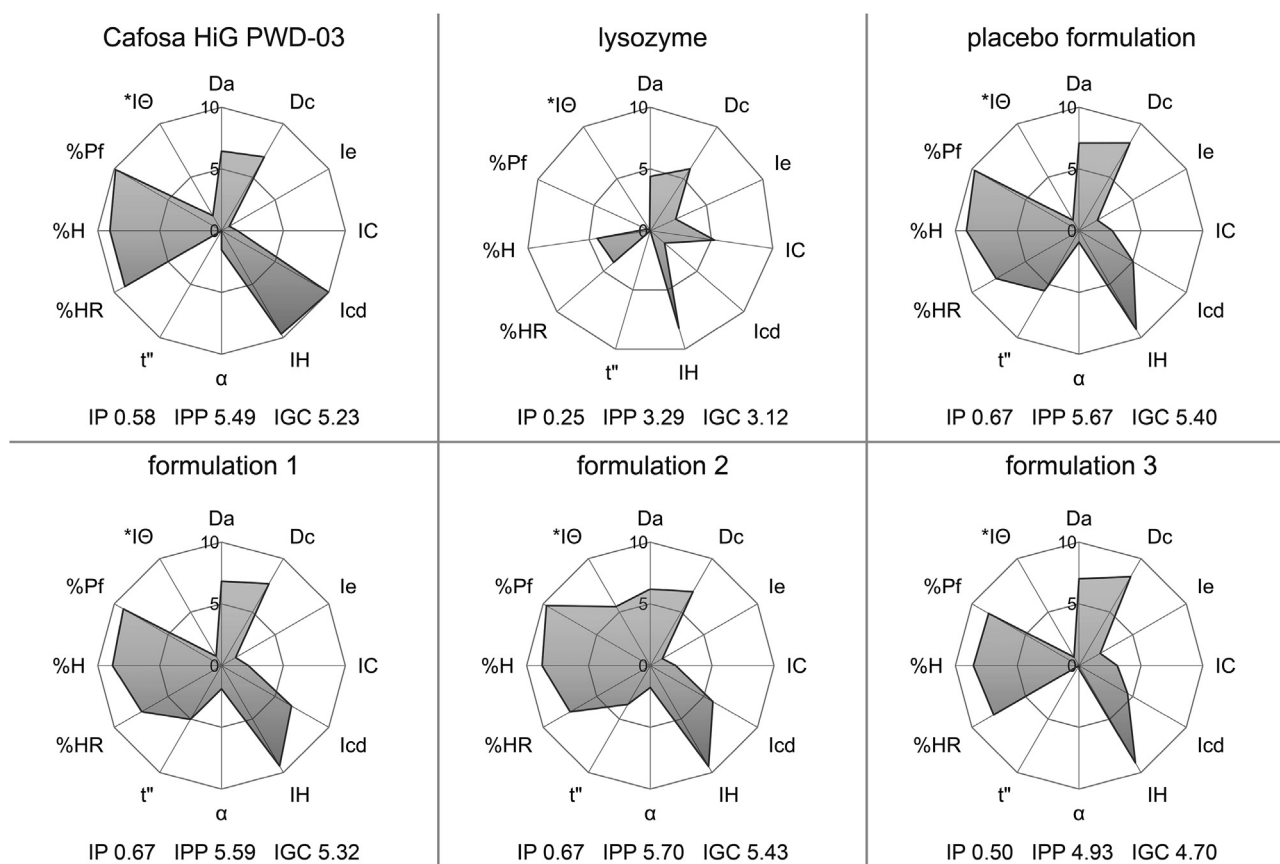


**Fig. 2.** SeDeM-Diagrams of the tested powdered substances and formulations. SeDeM-Diagram with 12 tested parameters for Cafosa HiG PWD-03, placebo formulation and formulation 1, 2, 3 and 11 parameters for lysozyme ( $\alpha$  angle of repose was excluded). Acceptance indexes are shown as parameter index (IP), parameter profile index (IPP) and good compressibility index (IGC).

obtained after the tablet broke.

**2.2.3.5. Release test.** In the European Pharmacopoeia the release testing of a drug substance from MCG is referred to as “dissolution test for medicated chewing gums”. However, no dissolution of the drug product occurs since the MCG is not disintegrating, but forms an elastic, chewable mass from which the API is released. Therefore this article will use the term “release test” to describe the performance test for MCG [34]. The performance of the MCG was tested for three chewing gums of formulations 1 to 3, respectively. The *in vitro* release testing of lysozyme-loaded chewing gums was operated based on the Ph. Eur. 2.9.25. “dissolution test for medicated chewing gums”, apparatus B in 40 mL phosphate buffer pH 6.0 R2 [32,35]. The apparatus applies mechanical force to the chewing gum by vertically moving the lower jaw combined with rotation of the upper jaw with agitation of the release medium (Fig. 4) [35]. The parameters were set to 1.65 mm for the jaw distance, 40° for the twisting angle and 30 chews per minute for the chewing frequency. The chewing gums were placed in the chewing chamber between two nets for fixation during the mastication process and equilibrated for 15 min before starting the chewing for a total time of 20 min at  $37 \pm 0.5$  °C. After predetermined time points, 1 mL of drug release medium was removed, filtered and replaced with fresh medium. Filtering was done with regenerated cellulose filters (pore size 0.22  $\mu$ m, diameter 13 mm, Spartan, Whatmann) after the filter was conditioned with 0.5 mL of medium. The sample solutions of chewing gums from formulations 1 and 2 were analysed directly, whereas the sample solutions of chewing gums from formulation 3 were diluted 1:2 with phosphate buffer pH 6.0 prior to the test. The HPLC analysis was conducted as described in Section 2.2.3.6.

**2.2.3.6. HPLC analysis.** The HPLC-System 2695 (Waters, Eschborn, Germany) with a reverse phase xBridge C18 column (length 15 mm, diameter 4.6 mm, pore size 3.5  $\mu$ m; Waters, Eschborn, Germany) was connected to a photodiode array (PDA) detector 2996 (Waters, Eschborn, Germany), at 280 nm. Further information on the method can be found in the [supplementary material](#) section (Fig. S3 and Table S2).

### 3. Results & discussion

#### 3.1. Powder characterisation and application of the SeDeM-Diagram-Expert-System to chewing gum formulations

The SeDeM-System has been developed to characterise powder properties for tablet formulations and to indicate whether the active substance, excipients or blends are suitable for direct compression [16]. In this study, the system was applied to directly compressed chewing gums with lysozyme as sensitive active substance. In contrast to standard tableting mixtures, the chewing gum formulation consists of a highly inhomogeneous and cohesive gum base [12,13]. The cohesive behaviour of the gum base, resulting in insufficient flow behaviour, was improved by adding lubricants to produce the placebo formulation. The basic blend with a targeted drug load of 5% of lysozyme was prepared and the influence of lysozyme in formulation 1 was compared with the placebo formulation. Effects on the powder properties by altering the particle size of the gum base were shown by preparing formulation 2, consisting of gum base with a main particle size of 100–355  $\mu$ m. The influence of the drug load for MCG manufactured by direct compression was shown by formulation 3, with a lysozyme content of 15%. The differences of the particles of the ingredients and the formulations were

**Table 2**

**Physical attributes of directly compressed chewing gums.** Chewing gum characteristics after compression of chewing gum formulations with an eccentric tableting machine. Unless otherwise specified, 10 samples were tested and the arithmetic mean  $\pm$  standard deviation is shown.

	Formulation 1	Formulation 2	Formulation 3
Diameter [mm]	18.03 $\pm$ 0.02	18.02 $\pm$ 0.01	18.16 $\pm$ 0.03
Height [mm]	5.84 $\pm$ 0.02	5.75 $\pm$ 0.01	5.99 $\pm$ 0.01
Mass [g]	1.65 $\pm$ 0.02	1.50 $\pm$ 0.01	1.58 $\pm$ 0.01
Breaking strength [N]	83 $\pm$ 5	54 $\pm$ 2	13 $\pm$ 3
Friability*	complied (0% abrasion)	complied (0% abrasion)	failed (100% broken)
Content [%]**	94.8 $\pm$ 7.7	96.4 $\pm$ 1.7	101.6 $\pm$ 1.8

\* n = 3, 10 samples were tested in one run.

\*\* n = 6.

visualized by stereo microscopy, VPSEM and confocal Raman microscopy (Fig. 1). Stereo microscopic images of the gum base revealed a broad particle size distribution, which was also observed in the placebo blend as well as in formulations 1 and 3 and was confirmed by sieve analysis (Fig. S1). In comparison, formulation 2 showed a narrow particle size distribution, since the gum base was sieved before blend manufacturing. The lysozyme powder was found to be homogenous in stereo microscopic images, with 85% particles < 100  $\mu$ m, as found in sieve analysis (Fig. S1) and supported by VPSEM (Fig. 1). The VPSEM images of the gum base revealed a rough particle surface which appeared smoothed after blending with excipients, resulting in the placebo formulation. Moreover, the images show lysozyme spheres, which were attached to the gum base particles in formulations 1–3. Confocal Raman microscopy supported this finding by identification of lysozyme attached to the gum base particles. Differences of the lysozyme amount can be found in comparison of formulations 1 and 2 with formulation 3. The findings of the visualised individual ingredients and formulations were compared to the powder properties characterised using the methods summarized in Table 1 and subsequently the SeDeM-System was applied as described in Section 2.2.4 (Table S1). The calculated SeDeM-Diagrams and the corresponding acceptance indexes, which allow for evaluation of direct compressibility, are presented in Fig. 2. The r values and acceptance indexes of the gum base, placebo formulation, as well as formulations 1–3 are clearly higher than the values for lysozyme. The higher the r values of the tested parameters, the larger the grey coloured area in the SeDeM-Diagram, as well as the acceptance indexes and the more likely the powder is suitable for direct compression. Arranging the powders by the number of r values above 5 in decreasing order, the placebo formulation, formulations 1 and 2 are followed by the gum base, formulation 3 and lysozyme (Fig. 2). Since the r values of the parameters are needed to calculate the acceptance indexes, the powders follow the same order and the values for the acceptance indexes also decrease. The raw gum base is suitable for direct compression as indicated by the acceptance indexes, although no flow ( $t''$ ) of the gum base was observed. For an automated tableting process, the raw chewing gum base would not be suitable for direct compression, but the highly cohesive chewing gum base also influences the parameters which affect the acceptance index, which indicates suitability for direct compression. Solely concerning the compression process, the compressibility of the raw gum base is given but in context of an automated tableting process, the parameter flow ( $t''$ ) needs to be improved by excipients. After addition of excipients to improve the flowability and lubrication, the resulting placebo formulation showed an improved flow ( $t''$ ) but also a decreased cohesion index (Icd). In comparison, lysozyme showed low acceptance indexes, indicating the need to add excipients for direct compression, as suggested by the SeDeM-System [17]. After blending lysozyme with the gum base and excipients to produce formulation 1, the above mentioned characteristics of lysozyme were indicated by a decrease of the r values of the

placebo formulation in the SeDeM-Diagram (Fig. 2). Overall, the acceptance indexes of formulation 1 point to appropriate powder characteristics for direct compression. The increase of the lysozyme content from 5% to 15% in formulation 3, leads to a further decrease of the r values in the SeDeM-Diagram. In particular, the flow and cohesion indexes are deteriorated. The overall acceptance indexes of formulation 3 were below the limit for direct compression. For formulations 1 and 2, differences in the particle size distribution of the chewing gum base were observed and the SeDeM-Diagram revealed disadvantages, which were associated with the narrow particle size distribution of the gum base from formulation 2 (100 – 355  $\mu$ m) (Fig. S1). Although the homogeneity index ( $*I\theta$ ) increased and the acceptance indexes were the highest compared to the other blends, the flowability ( $t''$ ) and cohesion index (Icd) were lowered. It can be concluded that additional particles below 100  $\mu$ m and above 355  $\mu$ m are positively influencing the flowing properties and cohesive properties of the gum base. In general, the particle size ratio of the gum base to the active substance shows a great influence on the blend behaviour during the tableting process [36]. Although the homogeneity index ( $*I\theta$ ) of formulation 2 displays better properties than found for formulations 1 and 3 in the corresponding SeDeM-Diagrams (Fig. 2), the content analysis of individual samples of the batch revealed only a minor difference in variability between formulations 2 and 3, indicating that lysozyme is homogeneously distributed within the blend (Table 2). This discrepancy of homogeneity index and content analysis of the batch might be due to the underlying assumption of the SeDeM-System, that a Gaussian distribution of the particle size should be observed. Additionally, 60% of the particles should be found in the middle fraction of the sieve-range used, in order to achieve homogeneously distributed API within the batch of the final product [17]. In the case of particles with a size below 100  $\mu$ m, this phenomenon could be explained by the formation of interactive mixtures with large particles of the matrix, resulting in stable and homogenous blends but with the possibility of unfavourable flow characteristics [13,24]. However, since lysozyme powder showed deficient flow properties due to electrostatic interaction with surfaces and consists of particles below 100  $\mu$ m, the formation of interactive mixtures, when blended with the highly cohesive gum base, is assumed. VPSEM and confocal Raman microscopy revealed lysozyme spheres being attached to the rough surface of the gum base particles (Fig. 1). Although the quantification of the lysozyme fraction, attached to the gum base particles was not possible, an increase of spheres was observed when comparing formulations 1 and 2 to formulation 3 (Fig. 1). Furthermore, the excipients used in all formulations seem to facilitate the interaction of gum base particles and lysozyme spheres, as can be observed in the VPSEM images. The excipients might support the adhesion of lysozyme spheres to the gum base particles by coating and stabilizing the agglomerates during the mixing process and thus assure the homogenous distribution in the blend as well as in the individual chewing gum tablets. The aforementioned findings indicate that the SeDeM-System is sensitive for formulation changes of direct compressible chewing gum tablets and imply the suitability of the SeDeM-System for prediction of direct compressibility. This hypothesis was subsequently tested by manufacturing and characterising chewing gum tablets of the corresponding formulations.

### 3.2. Chewing gum tablet properties

After manufacturing directly compressed chewing gum tablets, by keeping the compression force and filling depth of the tableting machine constant, ten individual gums of formulations 1–3 were investigated for differences in dimension and physical strength, influenced by the powder properties (Table 2). Since the tableting is a volume controlled process, the dimension parameters Da and Dc of the SeDeM-Diagram describe the powder properties, which influence the tablet dimensions. Due to a higher bulk density (Da), more powder fills the die of the tableting machine, resulting in tablets with increased

tablet height. Besides bulk density, elastic relaxation after the compression process can also lead to tablets with increased dimensions, especially in the case of chewing gum base with its plastic-elastic properties. This phenomenon has been investigated by monitoring the forces occurring during the tableting process of directly compressible chewing gum tablets [37]. In our study the height of chewing gum tablets produced from formulations 1–3 (Table 2) indicate a correlation with the bulk density (Fig. 2). Furthermore, the increased diameter of the chewing gum tablets from all three formulations is a result of elastic relaxation (Table 2). The largest diameter was observed with tablets manufactured from formulation 3 and could be linked to the higher lysozyme loading. This finding indicates strong elastic properties of the lysozyme powder, which influenced the tablet dimensions after force was applied during compression. However, it was not possible to distinguish between the predominant influence of the bulk density and the elastic properties of the powder on the tablet dimensions. Opposed to that, larger chewing gum tablets do not necessarily result in an increased weight. The different composition of the tablets had a greater influence on the packing density and therefore the chewing gum mass. Lysozyme had a low bulk density ( $D_a$ ) (Fig. 2) and the amount in formulation 3 was three times higher than in formulation 1, resulting in tablets with larger dimensions but decreased mass (Table 2). Formulations 1 and 2 with the same drug load showed differences in the tablet mass. Due to different particle size distributions in both formulations, smaller gum base particles, still present in formulation 1, might have filled the free inter-particle space, leading to a higher packing density in chewing gum tablets (Table 2). The combination of dimension and mass is supporting the finding of the different breaking strengths, since formulation 1 with the highest mass also results in the highest breaking strength followed by formulations 2 and 3 (Table 2). The cohesion indexes ( $I_{cd}$ ) of formulations 1–3 from the SeDeM-Diagram (Fig. 2) already indicated effects on the breaking strength of the chewing gum tablets and a clear impact on tablet hardness became apparent after the friability testing (Table 2). Furthermore, the acceptance indexes, which indicate the suitability for a powder to be directly compressible, matched the results of the friability. In fact, it was possible for all the formulations to be compressed with the tableting machine and result in chewing gum tablets which appeared acceptable by organoleptic analysis (Fig. 3A). Our findings support the assumption, that for chewing gum tablets, the SeDeM-System allows prediction of the mechanical attributes of the finished gum tablet. The prediction of the suitability of a chewing gum blend for direct compression needs to be further investigated, since the chewing gum mass is highly cohesive and likely to form tablets when it is compressed. Compared to disintegrating tablets, the prediction of the mechanical attributes is not sufficient to obtain a chewable chewing gum, which represents the activated state of this dosage form. The solid, glassy and inactivated chewing gum tablet however is activated by mastication and is transformed into the rubbery, elastic chewing gum, which is crucial for the performance of the dosage form and a prerequisite for the release mechanism [9,11]. To determine the performance of the chewing gum tablets compressed from the formulations characterised by the SeDeM-System, apparatus B was used, as described in Ph. Eur. (Fig. 4) [35]. The device is generating constant mechanical agitation comparable to the physiological mastication process and allows for release testing *in vitro*. Chewing gum tablets of formulations 1–3 showed initial crumbling under the conditions of the *in vitro* release test, before a coherent gum mass was built up by the instrument. Unlike formulations 1 and 2, formulation 3 consisted of 82% gum base, which resulted in the chewing gum tablet behaving more like a classical disintegrating tablet with fragmentation in the initial phase of mechanical exposure and the highest maximum release. The crumbling was also visible in the release profile as an initial burst effect (Fig. 5), which has been found to be typical for directly compressed chewing gum tablets [10]. The maximum release of formulations 1 and 2 at the end of the test was lower, presumably due to a faster gum formation during the initial phase of the

*in vitro* release test by embedding of the API in the gum base matrix under the influence of mechanical forces. The variability of the *in vitro* release profiles of the chewing gum tablets (Fig. 5) confirmed the results of the content uniformity analysis of the corresponding formulations. Nevertheless, formulation 1 showed a homogenous distribution of lysozyme within the chewing gum base on the surface as well as in the cross-section of the individual MCG visualized by confocal Raman microscopy analysis (Fig. 3B and C), whereas the uniformity of content analysis, with six chewing gum tablets, revealed a relatively high heterogeneity in the blend (Table 2). The chewing gum tester allows for the proof of similarity and differences within one formulation variant but also between different formulation variants as a result of formulation attributes. Additionally, the results of the release test show the significance of the mechanical properties of the chewing gum tablet on the release behaviour of the API from the gum matrix. Furthermore, the SeDeM-System allowed for the prediction of direct compressibility of chewing gum tablets from formulations 1 and 2 but failed to make predictions in the case of formulation 3. Only by the addition of testing for friability it was possible to identify a lack of mechanical stability of the chewing gum tablets produced from formulation 3. Besides sufficient mechanical stability, the chewability, which influences the performance of the chewing gum, is an essential prerequisite and defined by the QTPP. Therefore, the chewability needs to be considered in the early developmental stage as part of the CQA. It is possible to differentiate chewable chewing gum tablets from non-chewable chewing gum tablets with experimental tests [38]. Hagbani et al. provided an overview of non-compendial methods to test and evaluate the mechanical properties of chewing gum tablets, thereby predicting the chewability from the inactive form. In the present study, the MCG have been further characterised after the manufacturing process by investigation of physical properties and *in vitro* performance of both, the inactive and active form. It has been possible to distinguish between chewing gum tablets behaving like a brittle tablet and chewing gum tablets, which form a chewable mass while masticating, thus predicting the chewability of chewing gum tablets from the inactivated drug product [2]. Such a parameter could complete the SeDeM-System for chewing gum tablets to not only predict the suitability for direct compression, but also to set up a design space and define the maximum loading capacity to preserve the chewability of the chewing gum tablet.

#### 4. Conclusion

In this study, the SeDeM-System for development and optimisation of tablet formulations was successfully applied to chewing gum tablets. The QbD approach, exerted by the SeDeM-System, demonstrated sufficient discriminatory power to detect even minor changes in the tested formulations, even though the chewing gum base differs from typically used binders and fillers for direct compression of tablets. Although, it was possible to manufacture chewing gum tablets from a formulation with predicted unsuitability for direct compression, the samples of this formulation showed decreased physical stability and impaired transition from solid to elastic consistency. The limitation of the SeDeM-System for rational development of chewing gum tablet formulations is reflected in the unique properties of this dosage form. In the case of the formulations investigated in this study, a non-linear relationship between drug load and blend properties is assumed, which might be due to morphology and cohesive nature of the gum base. The possibility of the non-linear behaviour of powder blends should be considered in general, when applying the SeDeM-System. Especially if proteins are included as API, the interaction with the blend matrix needs further investigations and comparison to small molecules. Furthermore it can be concluded, that there is still a missing link between enhanced formulation development using the SeDeM-System for the manufacturing of the solid dosage form and the performance of the proactively activated chewing gum tablet. Meaningful inclusion of these parameters as part of the CMAs in the SeDeM-System to meet the specifications of the

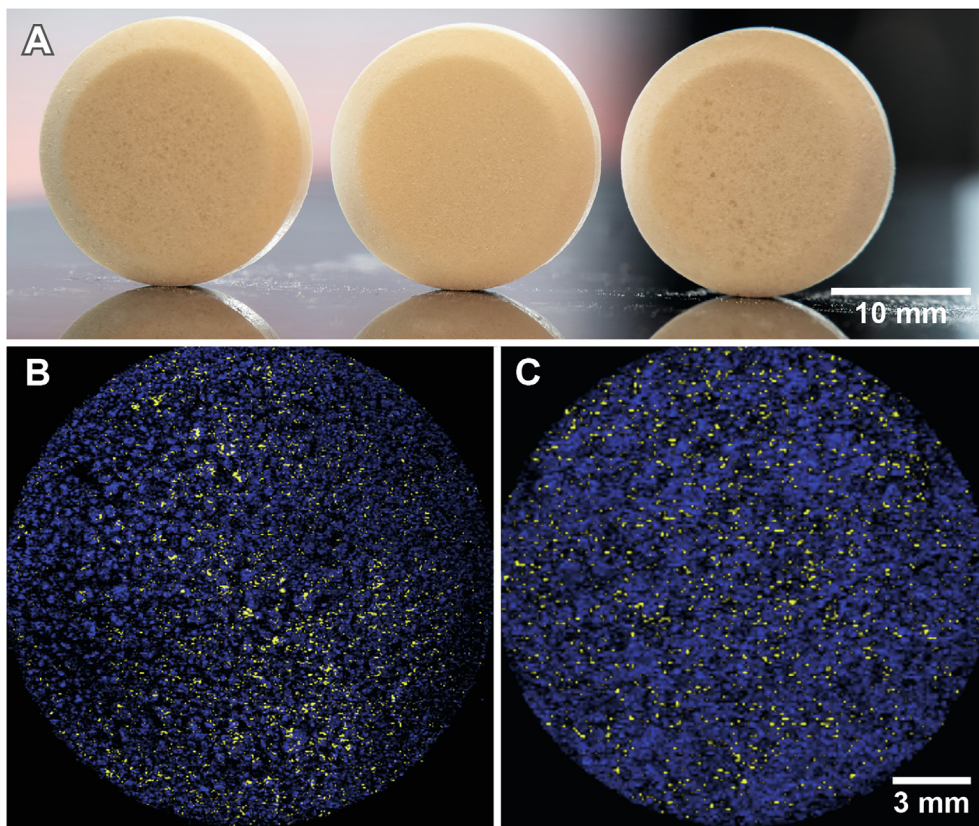


**Fig. 3.** Directly compressed lysozyme chewing gums (A) and confocal Raman microscope images of the chewing gum surface (B) and cross section (C). Representative photograph of lysozyme loaded chewing gums manufactured by direct compression using an eccentric tableting machine of formulation 1, 2 and 3 (from left to right) (A). Chemically selective analysis of the distribution of lysozyme (yellow) within the gum base matrix (blue) by confocal Raman microscopy on the gum base surface (B) and in the cross-section (C) of formulation 1. (For interpretation of the references to colour in this figure legend, the reader is referred to the web version of this article.)

CQAs could be beneficial to consider the special requirements for chewing gum formulations to fulfil the QTPP. Such a system would provide a sophisticated connection and understanding of the formulation process and performance of directly compressed chewing gum tablets, to comply with the requirements requested by the QbD concept.

**Declaration of Competing Interest**

The authors disclosed no conflicts of interest related to this article.

**Acknowledgements**

The authors thank Alisa Goutach for assistance with the experiments for powder characterisation, Matthias Opitz and Stephan Hollomotz from PHAST Development GmbH & Co. KG for their expertise in variable pressure scanning electron microscopy and Cafosa Health in Gum® for their kind support.

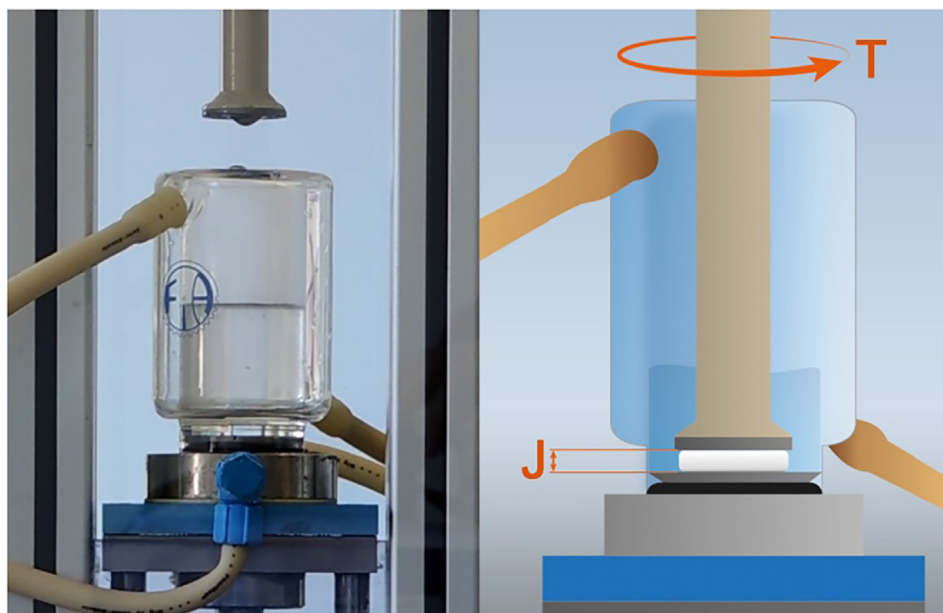


**Fig. 4.** Test chamber of the chewing gum tester (apparatus B) [35]. Photographic image (left) of the heatable, double-walled glass chamber, filled with release medium and schematic representation (right) with test chamber and a chewing gum sample placed between upper and lower jaw, with jaw distance (J) and twisting angle (T) of apparatus B [35].

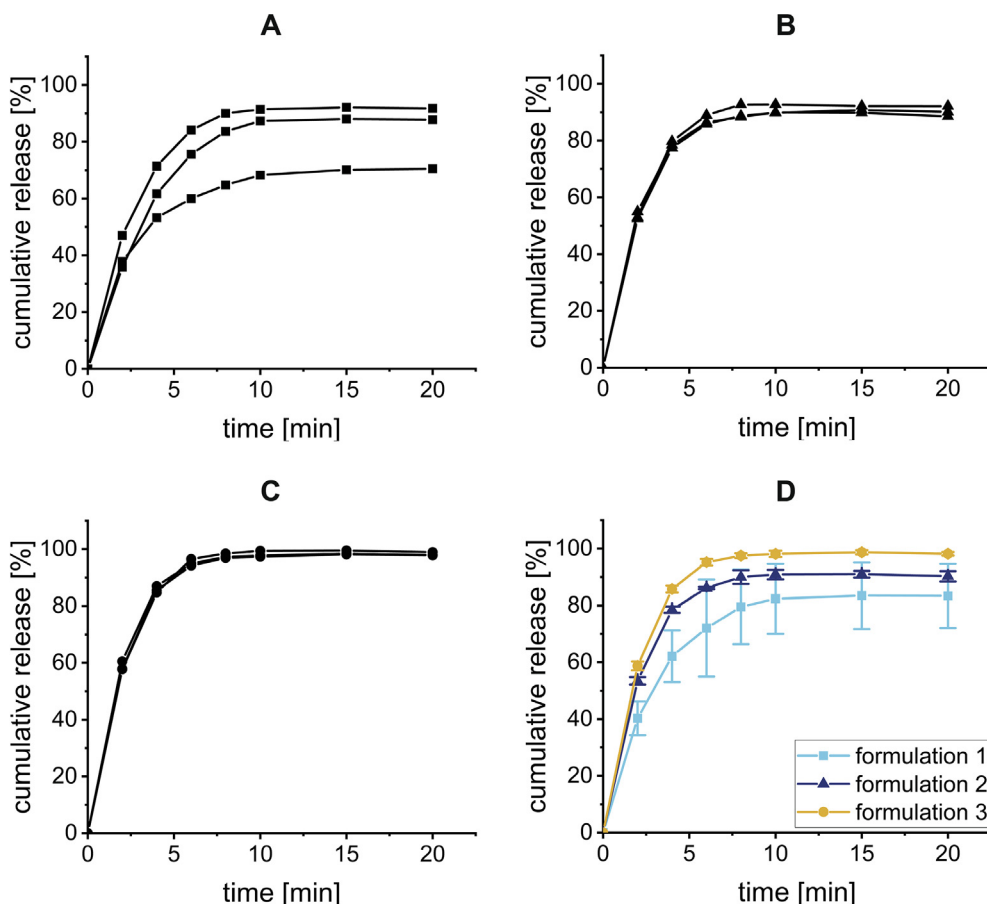


**Fig. 5. Release of lysozyme from different chewing gum formulations.** Cumulative release profile of lysozyme from directly compressed chewing gums from formulations 1 (A), 2 (B), 3 (C), and arithmetic mean (D) of chewing gums from three formulations, respectively and standard deviation as error bars ( $n = 3$ ). Results were obtained by using apparatus B [35] with the following settings; pre-heating time 15 min, temperature  $37 \pm 0.5^\circ\text{C}$ , volume 40 mL, sample 1 mL (replaced), twisting angle  $40^\circ$ , jaw distance 1.65 mm, chewing frequency 30 chews per min.

## Appendix A. Supplementary material

Supplementary data to this article can be found online at <https://doi.org/10.1016/j.ejpb.2019.09.003>.

## References

- N. Konar, I. Palabiyik, O.S. Toker, O. Sagdic, Chewing gum: Production, quality parameters and opportunities for delivering bioactive compounds, *Trends Food Sci. Tech.* 55 (2016) 29–38, <https://doi.org/10.1016/j.tifs.2016.07.003>.
- T. Al Hagbani, S. Nazzal, Medicated chewing gums (MCGs): composition, production, and mechanical testing, *AAPS PharmSciTech* 49 (2018) 30–37, <https://doi.org/10.1111/jtxs.12287>.
- M.R. Rassing, Chewing gum as a drug delivery system, *Adv. Drug Deliver. Rev.* 13 (1994) 89–121.
- S.A. Chaudhary, A.F. Shahiwal, Medicated chewing gum - a potential drug delivery system, *Expert Opin. Drug Del.* 7 (7) (2010) 871–885, <https://doi.org/10.1517/17425247.2010.493554>.
- J. Jacobsen, L.L. Christrup, N.-H. Jensen, Medicated chewing gum, *Am. J. Drug Del.* 2 (2) (2004) 75–88, <https://doi.org/10.2165/00137696-200402020-00001>.
- L. Zieschang, M. Klein, J. Krämer, M. Windbergs, In vitro performance testing of medicated chewing gums, *Dissolut. Technol.* 25 (3) (2018) 64–69, <https://doi.org/10.14227/DT250318P64>.
- < 1151 > Pharmaceutical dosage forms, in: *The United States Pharmacopeial Convention (Ed.), United States Pharmacopeia and National Formulary: USP 41-NF 36*, Rockville, MD, 2018, 1543–1568.
- Chewing gums, Medicated, in: *European Pharmacopoeia*, 9th ed., European Directorate for the Quality of Medicines, Council of Europe, Strasbourg, FR, 2016, pp. 855.
- J. Gajendran, Performance of medicated chewing gums with the goal of establishing in vitro in vivo correlation. PhD Thesis, Mainz, Germany, 2016.
- Y. Morjaria, W.J. Irwin, P.X. Barnett, R.S. Chan, B.R. Conway, In vitro release of nicotine from chewing gum formulations, *Dissolut. Technol.* 11 (2004) 12–15, <https://doi.org/10.14227/DT110204P12>.
- J. Gajendran, J. Kraemer, P. Langguth, In vivo predictive release methods for medicated chewing gums, *Biopharm. Drug Dispos.* 33 (2012) 417–424, <https://doi.org/10.1002/bdd.1796>.
- J. Belmar, M. Ribé, Eye on excipients: Direct compression of medicated chewing gum, *Tablets & Capsules [Online]*, 2013, pp. 1–4, <http://www.healthgum.com/pdf/Eye%20on%20excipients> (accessed 18 June 2018).
- W.A. Ritschel, A. Bauer-Brandl, *Die Tablette: Handbuch der Entwicklung, Herstellung und Qualitätssicherung*, 2., vollst. überarb. und erw. Aufl. ed., ECV - Editio-Cantor-Verl., Aulendorf, 2002.
- International Conference on Harmonisation of Technical Requirements for Registration of Pharmaceuticals for Human use, *Pharmaceutical Development Q8(R2)*, 4th ed., 2009.
- J.M. Suñé Negre, M. Roig Carreras, R. Fuster García, C.R. Hernández PérezRuhí Roura, E. García Montoya, M. Miñarro Carmona, P. Pérez Lozano, J.R. Ticó Grau, Nueva metodología de preformulación galénica para la caracterización de sustancias en relación a su viabilidad para la compresión: Diagrama SeDeM, *Ciencia Y Tecnología Farmacéutica* 15 (3) (2005) 125–136.
- P. Pérez, J.M. Suñé-Negre, M. Miñarro, M. Roig, R. Fuster, E. García-Montoya, C. Hernández, R. Ruhí, J.R. Ticó, A new expert systems (SeDeM diagram) for control batch powder formulation and preformulation drug products, *Eur. J. Pharm. Biopharm.* 64 (2006) 351–359, <https://doi.org/10.1016/j.ejpb.2006.06.008>.
- J.M. Suñé Negre, E. García Montoya, P. Pérez Lozano, J.E. Aguilar Díaz, M. Roig Carreras, R. Fuster García, M. Miñarro Carmona, J.R. Ticó Grau, SeDeM Diagram: A New Expert System for the Formulation of Drugs in Solid Form, in: *InTech (Ed.), Expert Systems for Human, Materials and Automation*, InTech, 2011.
- J.M. Suñé-Negre, P. Pérez-Lozano, M. Miñarro, M. Roig, R. Fuster, C. Hernández, R. Ruhí, E. García-Montoya, J.R. Ticó, Application of the SeDeM Diagram and a new mathematical equation in the design of direct compression tablet formulation, *Eur. J. Pharm. Biopharm.* 69 (2008) 1029–1039, <https://doi.org/10.1016/j.ejpb.2008.01.020>.
- E. Sipos, A.R. Oltean, Z.-I. Szabó, E.-M. Rédi, G.D. Nagy, Application of SeDeM expert systems in preformulation studies of pediatric ibuprofen ODT tablets, *Acta Pharmaceut.* 67 (2017) 237–246, <https://doi.org/10.1515/acph-2017-0017>.
- J.E. Aguilar-Díaz, E. García-Montoya, J.M. Suñé-Negre, P. Pérez-Lozano, M. Miñarro, J.R. Ticó, Predicting orally disintegrating tablets formulations of ibuprofen tablets: an application of the new SeDeM-ODT expert system, *Eur. J. Pharm. Biopharm.* 80 (2012) 638–648, <https://doi.org/10.1016/j.ejpb.2011.12.012>.
- J.E. Aguilar-Díaz, E. García-Montoya, P. Pérez-Lozano, J.M. Suñé-Negre, M. Miñarro, J.R. Ticó, The use of the SeDeM Diagram expert system to determine the suitability of diluents-disintegrants for direct compression and their use in formulation of ODT, *Eur. J. Pharm. Biopharm.* 73 (2009) 414–423, <https://doi.org/10.1016/j.ejpb.2009.07.001>.
- A. Khan, Z. Iqbal, Z. Rehman, F. Nasir, A. Khan, M. Ismail, Roohullah, A. Mohammad, Application of SeDeM Expert system in formulation development of effervescent tablets by direct compression, *Saudi Pharm. J.* 22 (2014) 433–444,

- <https://doi.org/10.1016/j.jsps.2013.07.002>.
- [23] J.M. Suñé-Negre, M. Roig, R. Fuster, C. Hernández, R. Ruhí, E. García-Montoya, P. Pérez-Lozano, M. Miñarro, J.R. Ticó, New classification of directly compressible (DC) excipients in function of the SeDeM Diagram Expert System, *Int. J. Pharm.* 470 (2014) 15–27, <https://doi.org/10.1016/j.ijpharm.2014.04.068>.
- [24] J.C. Scholtz, J.H. Steenekamp, J.H. Hamman, L.R. Tiedt, The SeDeM Expert Diagram System: Its performance and predictability in direct compressible formulations containing novel excipients and different types of active ingredients, *Powder Technol.* 312 (2017) 222–236, <https://doi.org/10.1016/j.powtec.2017.02.019>.
- [25] E. Galdón, M. Casas, M. Gayango, I. Caraballo, First study of the evolution of the SeDeM expert system parameters based on percolation theory: monitoring of their critical behavior, *Eur. J. Pharm. Biopharm.* 109 (2016) 158–164, <https://doi.org/10.1016/j.ejpb.2016.10.004>.
- [26] S. Dai, B. Xu, G. Shi, J. Liu, Z. Zhang, X. Shi, Y. Qiao, SeDeM expert system for directly compressed tablet formulation: a review and new perspectives, *Powder Technol.* 342 (2019) 517–527, <https://doi.org/10.1016/j.powtec.2018.10.027>.
- [27] Bulk Density and Tapped Density of Powders. 2.9.34., in: *European Pharmacopoeia*, 9th ed., European Directorate for the Quality of Medicines, Council of Europe, Strasbourg, FR, 2016, pp. 359–361.
- [28] Powder Flow. 2.9.36., in: *European Pharmacopoeia*, 9th ed., European Directorate for the Quality of Medicines, Council of Europe, Strasbourg, FR, 2016, pp. 362–365.
- [29] I. Nofrerías, A. Nardi, M. Suñé-Pou, J. Boeckmans, J.M. Suñé-Negre, E. García-Montoya, P. Pérez-Lozano, J.R. Ticó-Grau, M. Miñarro-Carmona, Optimization of the cohesion index in the SeDeM diagram expert system and application of SeDeM diagram: an improved methodology to determine the cohesion index, *PLoS One* 13 (9) (2018) e0203846, <https://doi.org/10.1371/journal.pone.0203846>.
- [30] J.M. Suñé-Negre, P. Pérez-Lozano, M. Roig, R. Fuster, C. Hernández, R. Ruhí, E. García-Montoya, M. Miñarro, J.R. Ticó, Optimization of parameters of the SeDeM Diagram Expert System: Hausner index (IH) and relative humidity (%RH), *Eur. J. Pharm. Biopharm.* 79 (2011) 464–472, <https://doi.org/10.1016/j.ejpb.2011.04.002>.
- [31] Flowability. 2.9.16., in: *European Pharmacopoeia*, 9th ed., European Directorate for the Quality of Medicines, Council of Europe, Strasbourg, FR, 2016, pp. 321–322.
- [32] Phosphate buffer solution pH 6.0 R2, in: *European Pharmacopoeia*, 9th ed., European Directorate for the Quality of Medicines, Council of Europe, Strasbourg, FR, 2016.
- [33] Friability of uncoated tablets. 2.9.7., in: *European Pharmacopoeia*, 9th ed., European Directorate for the Quality of Medicines, Council of Europe, Strasbourg, FR, 2016, pp. 312–313.
- [34] C.K. Brown, H.D. Friedel, A.R. Barker, L.F. Buhse, S. Keitel, T.L. Cecil, J. Kraemer, J.M. Morris, C. Reppas, M.P. Stickelmeyer, C. Yomota, V.P. Shah, FIP/AAPS joint workshop report: dissolution/in vitro release testing of novel/special dosage forms, *AAPS PharmSciTech* 12 (2011) 782–794, <https://doi.org/10.1208/s12249-011-9634-x>.
- [35] Dissolution test for Medicated Chewing Gums. 2.9.25., in: *European Pharmacopoeia*, 9th ed., European Directorate for the Quality of Medicines, Council of Europe, Strasbourg, FR, 2016, pp. 340–344.
- [36] M. Leane, K. Pitt, G.K. Reynolds, N. Dawson, I. Ziegler, A. Szepes, A.M. Crean, R. Dall Agnol, The Manufacturing Classification System (MCS) Working Group (2018), Manufacturing classification system in the real world: factors influencing manufacturing process choices for filed commercial oral solid dosage formulations, case studies from industry and considerations for continuous processing, *Pharm. Dev. Technol.* 23 (2018) 964–977, <https://doi.org/10.1080/10837450.2018.1534863>.
- [37] I. Jójárt, The Importance of Magnesium Stearate in Pharmaceutical Industry and in the Preformulation Studies of Medicated Chewing Gums, PhD thesis, Szeged, 2014.
- [38] T. Al Hagbani, S. Nazzal, Development of postcompressional textural tests to evaluate the mechanical properties of medicated chewing gum tablets with high drug loadings, *J. Texture Stud.* 49 (2017) 1–8, <https://doi.org/10.1111/jtxs.12287>.